

Generation of 3.6 μm radiation and telecom-band amplification by four-wave mixing in a silicon waveguide with normal group velocity dispersion

B. Kuyken^{1,2*}, P. Verheyen³, P. Tannouri⁴, J. Van Campenhout³, R. Baets⁴, W. M. J. Green⁴, and G. Roelkens^{1,2}

¹*Photonics Research Group, Department of Information Technology, Ghent University - IMEC, Sint-Pietersnieuwstraat 41, 9000 Ghent, Belgium*

²*Center for Nano- and Biophotonics (NB-Photonics), Ghent University, Belgium*

³*imec, Kapeldreef 75, B-3001 Leuven, Belgium*

⁴*IBM T.J. Watson Research Center, 1101 Kitchawan Road, Yorktown Heights, NY 10598, USA*

**Corresponding author: Bart.Kuyken@intec.ugent.be*

Received Month X, XXXX; revised Month X, XXXX;
accepted Month X, XXXX; posted Month X, XXXX (Doc.
ID XXXXX); published Month X, XXXX

Mid-infrared light generation through four-wave mixing-based frequency down-conversion in a normal group velocity dispersion silicon waveguide is demonstrated. A telecom-wavelength signal is down-converted across more than 1.2 octaves using a pump at 2190 nm in a 1cm long waveguide. At the same time 13dB parametric gain of the telecom signal is obtained.

OCIS Codes: (130.3120) Integrated optics devices; (190.0190) Nonlinear optics;

The broadband transparency of the silicon-on-insulator waveguide platform from 1.1 μm (limited by the absorption of silicon) to $\sim 4\mu\text{m}$ (limited by the absorption of SiO_2) [1] enables the realization of photonic integrated circuits outside the telecommunication band. Such circuits can be valuable for spectroscopic sensing applications, which leverage the strong rovibrational absorption lines of molecules in the mid-infrared wavelength spectrum – the so-called molecular fingerprint region [2]. While silicon provides an excellent platform for passive waveguiding in this 1.1 - 4 μm wavelength range [1, 3], the generation and detection of mid-infrared radiation is not straightforward. Recent research has been geared towards the integration of III-V semiconductor devices onto the silicon photonics platform to implement this functionality [4, 5]. However, mid-infrared semiconductor photodetectors suffer from poor sensitivity at room temperature due to their narrow band gap, while semiconductor light sources only offer a limited gain bandwidth and hence a limited emission wavelength range. Efficient nonlinear optical effects on the silicon photonic platform, making use of the instantaneous third-order $\chi(3)$ nonlinear effect, can provide a solution to many of these challenges. Recent work has shown that four-wave mixing-based nonlinear optical functions including supercontinuum generation [6], optical parametric amplification [7, 8] and wavelength conversion [7-10] can be integrated for mid-infrared light generation within compact silicon photonic integrated circuits. Moreover, silicon waveguides accomplishing bi-directional broadband spectral translation of optical signals between 1620 nm and 2440 nm in the mid-infrared [11], and

between 1312 nm and 1884 nm in the short-wave infrared [12] have been demonstrated using four-wave mixing phase matched by anomalous dispersion. Such spectral translation technology can be applied to mid-infrared spectroscopic functions on a silicon photonic integrated circuit, by using advanced telecom-wavelength laser sources and high-sensitivity photodetectors. In this paper, we demonstrate that by using silicon waveguides with normal dispersion, the range of mid-infrared light generation and spectral translation can be extended to 3.6 μm wavelength, by frequency down-conversion across 1.2 octaves from the telecom band.

The spectral translator waveguide used in this work is dispersion engineered specifically to allow for phase matching far away from the pump wavelength. The phase matching condition for the degenerate four-wave mixing process is given by

$$\beta_2 \Delta\omega^2 + \frac{1}{12} \beta_4 \Delta\omega^4 + 2\gamma P = 0 \quad (1)$$

in which β_2 and β_4 are the second- and fourth-order dispersion coefficients of the silicon waveguide at the pump wavelength, γ is the nonlinear parameter of the waveguide ($\gamma = 20 \text{ (Wm)}^{-1}$ in the presented experiments) and P is the pump power. Depending on the signs of β_2 and β_4 , a variety of phase matching conditions near to and far away from the pump can be obtained. In our previous work [6-8,13], anomalously dispersive waveguides ($\beta_2 < 0$) with a positive β_4 were used, such that phase matching both close to the pump (broadband phase matching) and

far away from the pump (discrete band phase matching) could be observed simultaneously. In this paper air-clad silicon waveguides with a 400 nm thick silicon guiding layer and are designed to have normal dispersion and negative β_4 around a wavelength of ~ 2200 nm as illustrated in Figure 1(a) for the 1650 nm wide waveguide shown in the inset (assuming TE-polarized light). This dispersion design permits phase matching far away from the pump in the mid-infrared wavelength range. Figure 1(b) shows the simulated phase matched idler and signal wavelengths (in blue) as a function of pump wavelength for this waveguide. A peak pump power P of 20 W is assumed. The simulations indicate that phase matching between a signal at 1700 nm and an idler at 3076 nm can be obtained using a 2190 nm pump. The dispersion coefficients at 2190 nm are $\beta_2 = 3.67 \times 10^{-2} \text{ ps}^2/\text{m}$ and $\beta_4 = -4.78 \times 10^{-6} \text{ ps}^4/\text{m}$, respectively.

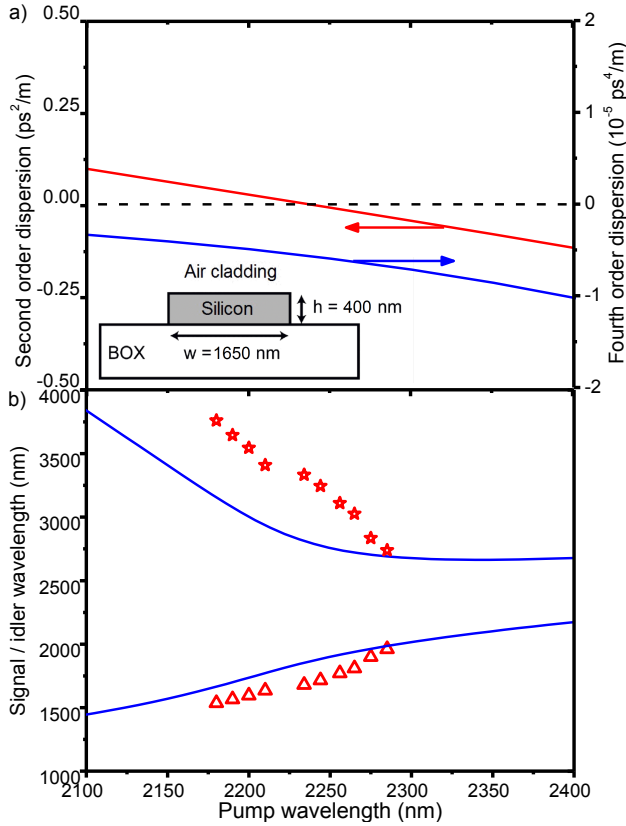


Figure 1: (a) The second- and fourth-order dispersion as a function of the pump wavelength for the waveguide geometry shown in the inset. The zero dispersion wavelength is at 2240 nm. The fourth-order dispersion is negative within the wavelength range of interest. (b) Phase-matched idler and signal wavelength as a function of pump wavelength. The blue curve shows the simulated phase matched wavelengths, for a peak pump power of 20 W. The red triangles label the positions of the experimentally observed modulation instability peaks on the blue side of the pump, while the red stars correspond to the energy-conserving wavelengths on the red side of the pump.

A series of four-wave mixing experiments are performed using a 1 cm long silicon waveguide. The waveguide is fabricated in imec's CMOS pilot line, on 200 mm silicon-

on-insulator wafers having a 400 nm thick silicon device layer on a 2 μm buried oxide layer (BOX). The propagation loss for the 1650 nm wide waveguides is measured through a cut-back measurement to be less than 0.2 dB/cm, at both telecom wavelengths and at the 2190 nm pump wavelength. Due to the lack of a suitable laser source, the propagation loss in the mid-infrared could not be evaluated. For the spectral translation experiments, a picosecond pulse train (FWHM of 2 ps, repetition rate of 76 MHz, generated from a Coherent MIRA Optical Parametric Oscillator) is used as the pump, which is coupled to the silicon waveguide using lensed fibers. The fiber-to-chip coupling loss at each facet is 8.5 \pm 1 dB, both at telecom wavelengths as well as at ~ 2190 nm. A telecom tunable continuous wave laser is used as an input probe signal. The signal and pump are combined using a 90/10 fused silica fiber coupler, and independent polarization controllers are used to launch TE-polarized light into the silicon waveguide.

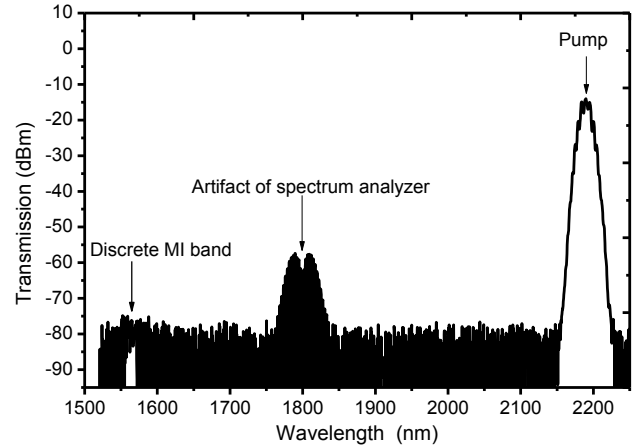


Figure 2: Spectrum at the output of the 1 cm long silicon waveguide. The pump pulses are centered at a wavelength of 2190 nm and have a coupled peak power of 20 W. The phase-matched amplification of background noise, i.e. the modulation instability effect, is seen in a discrete band around 1560 nm.

In a first experiment, the parametric fluorescence (i.e. parametric amplification of background noise, also referred to as modulation instability (MI) [14,15]) from the 1650 nm wide waveguide is characterized as a function of the pump wavelength, using a Yokogawa AQ6375 spectrum analyzer operating at 1 nm spectral resolution. Figure 2 shows the output spectrum obtained when the silicon waveguide is pumped with a pulse train centered at 2190 nm having a coupled peak power of 20 W. The spectral peak where phase matching occurs and background noise is amplified is labeled as the discrete MI band, and is centered around 1560 nm. This peak locates the signal wavelength for which perfect phase matching is obtained, according to Equation (1). The discrete MI band is the only band where phase matching occurs; the peak near 1800 nm is a known stray-light artifact within the spectrum analyzer. For waveguides designed with normal dispersion, there is no amplification of background noise near the pump, as is typically observed in silicon waveguides having anomalous dispersion [8]. This enormous reduction of amplified quantum noise (AQN) is

significant, because the AQN deteriorates the performance of a spectral translator [11–13].

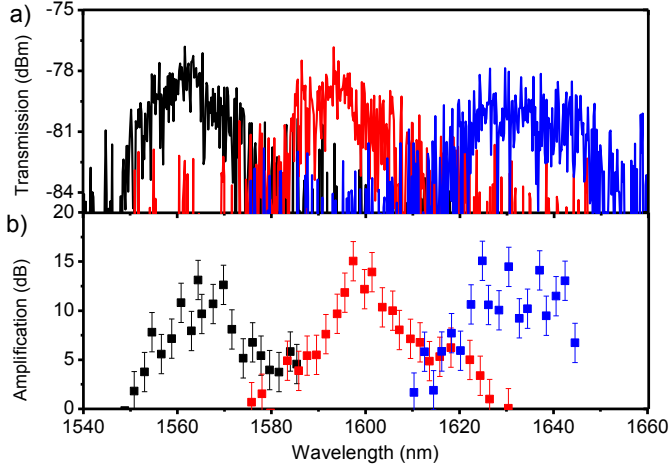


Figure 3: (a) Output spectra of the spectral translator device when only the pump is injected in the silicon waveguide, showing the position of the modulation instability side band for pump wavelengths of 2190 nm (black), 2200 nm (red) and 2210 nm (blue), with pump peak powers of 19.2 W, 18.3 W, 16.5 W respectively. (b) Corresponding gain spectra for each pump wavelength when the modulation instability band is probed.

Figure 3(a) shows a close-up of the output modulation instability spectra for pump wavelengths of 2190 nm, 2200 nm, and 2210 nm. As expected from the simulated curves in Figure 1, the signal wavelength where phase matching is achieved is highly dependent upon the pump wavelength. The peak of the sidebands shift from 1560 nm, to 1590 nm, and ultimately to 1630 nm, when the pump is tuned across the range from 2190 nm to 2210 nm, which allows to tune the phase matching bands [17]. The peak MI wavelengths observed on the blue side of the pump for all experiments performed are plotted as red triangles in Figure 1. Energy conservation is used to infer the position of the corresponding mid-infrared MI sidebands, as illustrated by the red stars.

An additional set of experiments are performed to characterize the four-wave mixing parametric gain as a function of input signal wavelength. By combining the pump with a low power tunable CW laser, the signal amplification across the short-wavelength modulation instability sideband is measured using a method similar to that described in [8]. Figure 3(b) plots the parametric amplification associated with the modulation instability sidebands shown in Figure 3(a). These experiments show that for peak pump powers of 19.2 W at a wavelength of 2190 nm, signals in a band around 1570 nm can be amplified by up to 15 dB. When the pump wavelength is tuned to 2200 nm, for which the peak power is 18.3 W, it is possible to amplify signals in a band around 1600 nm. Finally, when the pump is shifted another 10 nm to 2210 nm, with 16.5 W peak power, signals in a band around 1630 nm can be amplified. For a pump centered at 2210 nm, the measured amplification spectrum is more noisy because the OPO pulse train amplitude becomes less stable as the OPO is tuned to longer wavelengths. Nevertheless, the data in Figure 3(b) illustrates that

silicon spectral translator devices can also be used for amplification of telecom-wavelength signals.

Since parametric amplification is obtained at telecommunication wavelengths far away from the pump, a corresponding idler wave is generated in the mid-infrared. This was experimentally verified by characterizing the spectrum at the output of the spectral translator device, when both a telecom signal and a 2190 nm pump are injected simultaneously. Figure 4(a) shows a spectrum recorded with a Fourier Transform Infra-Red spectrometer (FTIR) and a liquid nitrogen cooled InSb detector, operating at 16 cm^{-1} resolution. A long-pass optical filter is used to attenuate the strong residual pump before coupling the transmitted light into the FTIR. The spectrum exhibits a generated mid-infrared idler at 3635 nm, seen above the detector's thermal background, when a 1565 nm signal is injected along with the 2190 nm pump. Varying the signal wavelength within the parametric gain bandwidth also shifts the mid-infrared idler. This is illustrated in Figure 4(b), which shows that idler waves are generated at 3635 nm, 3657 nm, 3677 nm, and 3696 nm, when telecom signals at 1565 nm, 1559 nm, 1554 nm, and 1550 nm, respectively, are injected together with the pump. This data illustrates the prospect of using silicon spectral translator devices for tunable mid-infrared light generation, based upon down-conversion of well-developed near-infrared tunable laser sources.

Silicon photonic integrated circuits may become a key technology for mid-infrared spectroscopic sensing applications that require low-cost and compact optical components. The unavailability of integrated light sources and photodetectors at these wavelengths is however hampering this development. Nonlinear optics on the silicon platform offers a promising solution to this problem, by providing a means for spectral translation of optical signals to and from the telecommunication wavelength range. In this paper, spectral translation across 1.2 octaves to the 3.6 μm wavelength range, which lies close to the edge of the silicon-on-insulator transparency window, is demonstrated using a silicon waveguide engineered specifically for normal dispersion. Furthermore, amplified quantum noise is suppressed in the normally dispersive silicon waveguide, since phase matching close to the pump is not possible. Extension further into the mid-infrared can be accomplished by modifying the waveguide cladding material, e.g. by moving to silicon-on-sapphire waveguide circuits [18,19] or free standing silicon [20], which would allow optical transparency up to 8 μm wavelength [1]. In addition to the demonstration of mid-infrared light generation, substantial telecom-wavelength optical amplification on a silicon chip is realized, illustrating that silicon nonlinear optical processes can also be useful for communication-oriented applications.

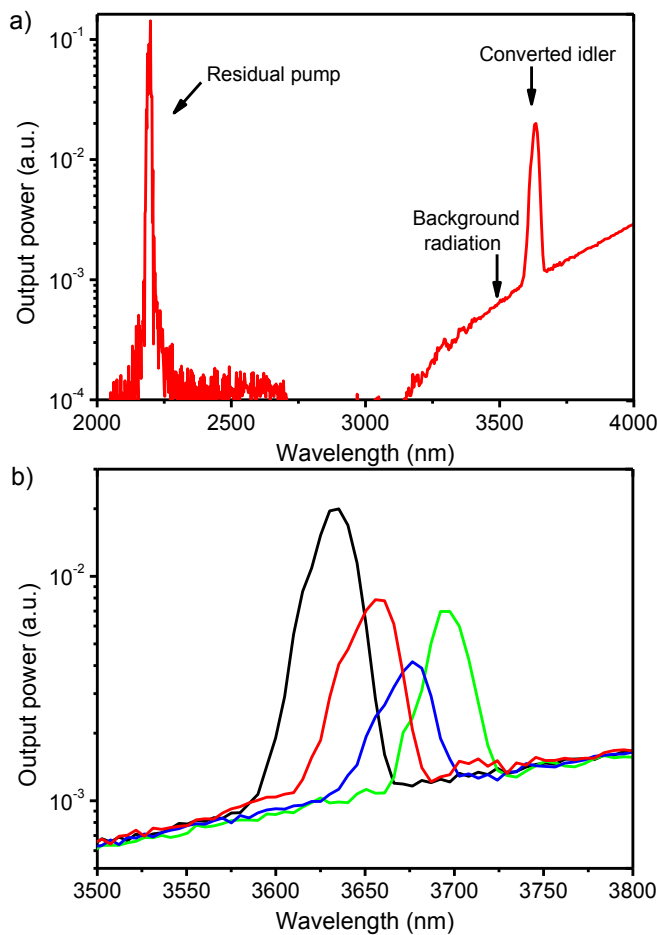


Figure 4. (a) Output spectrum recorded with an FTIR (16 cm^{-1} resolution) when the waveguide is pumped at 2190 nm with a peak power of 18.3 W, and probed by a telecom signal at 1565 nm. The converted idler is seen at 3635 nm, above the thermal background radiation signal. (b) Mid-infrared idler spectrum for telecom signal wavelengths of 1565 nm (black), 1559 nm (red), 1554 nm (blue), and 1550 nm (green).

Acknowledgements

This work was carried out in the framework of the FP7-ERC-MIRACLE project. Bart Kuyken acknowledges the Fund for Scientific Research (FWO-Vlaanderen) for a scholarship.

References

1. R. Soref, "Mid-infrared photonics in silicon and germanium," *Nat. Photon.* **4**, 495 (2010).
2. J. G. Crowder, S. D. Smith, A. Vass, J. Keddle, *Infrared methods for gas detection*, (Springer-Verlag, 2006).
3. M. M. Milosevic, M. Nedeljkovic, T. M., B. Masaud, E. Jaberansary, H. M. Chong, N.G. Emerson, G. Z. Mashanovich, "Silicon waveguides and devices for the mid-infrared," *Appl. Phys. Lett.* **101**, 121105 (2012).
4. N. Hattasan, A. Gassenq, L. Cerutti, J. Rodriguez, E. Tournié, G. Roelkens, "Heterogeneous Integration of GaInAsSb p-i-n Photodiodes on a Silicon-on-Insulator Waveguide Circuit," *IEEE Photon. Technol. Lett.* **23**, 1760 (2011).
5. N. Hattasan, A. Gassenq, L. Cerutti, J.B. Rodriguez, E. Tournié, G. Roelkens, "GaSb-based integrated lasers and photodetectors on a Silicon-On-Insulator waveguide circuit for sensing applications in the shortwave infrared," *Proceedings of Photonics Global Conference 2012*, Singapore, (2012).
6. B. Kuyken, X. Liu, R. M. Osgood Jr., R. Baets, G. Roelkens, W. M.J. Green, "Mid-infrared to telecom-band supercontinuum generation in highly nonlinear silicon-on-insulator wire waveguides," *Opt. Express* **19**, 20172 (2011).
7. X. P. Liu, R. M. Osgood, Y. A. Vlasov, and W. M. J. Green, "Mid-infrared optical parametric amplifier using silicon nanophotonic waveguides," *Nat. Photon.* **4**, 557 (2010).
8. B. Kuyken, X. Liu, G. Roelkens, R. Baets, R. M. Osgood, Jr., and W. M. J. Green, "50 dB parametric on-chip gain in silicon photonic wires," *Opt. Lett.* **36**, 4401 (2011).
9. R. K. W. Lau, M. Ménard, Y. Okawachi, M. A. Foster, A. C. Turner-Foster, R. Salem, M. Lipson, and A. L. Gaeta, "Continuous-wave mid-infrared frequency conversion in silicon nanowaveguides," *Opt. Lett.* **36**, 1263 (2011).
10. S. Zlatanovic, J. S. Park, S. Moro, J. M. C. Boggio, I. B. Divliansky, N. Alic, S. Mookherjea, and S. Radic, "Mid-infrared wavelength conversion in silicon waveguides using ultracompact telecom-band-derived pump source," *Nat. Photon.* **4**, 561 (2010).
11. X. Liu, B. Kuyken, G. Roelkens, R. Baets, R. M. Osgood Jr., W. M. J. Green, "Bridging the mid-infrared-to-telecom gap with silicon nanophotonic spectral translation," *Nat. Photon.* **6**, 667 (2012).
12. N. Ophir, R. K. W. Lau, M. Menard, R. Salem, K. Padmaraju, Y. Okawachi, M. Lipson, A. L. Gaeta, and K. Bergman, "First demonstration of a 10-Gb/s RZ end-to-end four-wave-mixing based link at 1884 nm using silicon nanowaveguides," *IEEE Photonics Technol. Lett.* **24**(4), 276-278 (2012).
13. F. Gholami, B. P.-P. Kuo, S. Zlatanovic, N. Alic, S. Radic, "Phase-preserving parametric wavelength conversion to SWIR band in highly nonlinear dispersion stabilized fiber," *Opt. Express* **31**, 11415 (2013).
14. B. Kuyken, X. Liu, R. M. Osgood, R. Baets, G. Roelkens, W. Green, "A silicon-based widely tunable short-wave infrared optical parametric oscillator," *Opt. Express* **21**, 5931 (2013).
15. J. D. Harvey, R. Leonhardt, S. Coen, G. K. L. Wong, J. C. Knight, W. J. Wadsworth, and P. S. J. Russell, "Scalar modulation instability in the normal dispersion regime by use of a photonic crystal fiber," *Opt. Lett.* **28**, 2225 (2003).
16. M. Yu, C. J. McKinstrie, and G. P. Agrawal, "Modulational instabilities in dispersion-flattened fibers," *Physical Review E* **52**, 1072 (1995).
17. Q. Lin, O. J. Painter, and G. P. Agrawal, "Nonlinear optical phenomena in silicon waveguides: modeling and applications," *Opt. Express* **15**, 16604 (2007).
18. T. Baehr-Jones, A. Spott, R. Ilic, A. Spott, B. Penkov, W. Asher, M. Hochberg, "Silicon-on-sapphire integrated waveguides for the mid-infrared," *Opt. Express* **18**, 12127 (2010).
19. F. Li, S.D. Jackson, C. Grillet, E. Magi, D. Hudson, S.J. Madden, D.J. Moss, "Low propagation loss silicon-on-sapphire waveguides for the mid-infrared," *Opt. Express* **19**, 15212 (2011).
20. R. Shankar, R. Leijssen, I. Bulu, and M. Loncar, "Mid-infrared photonic crystal cavities in silicon," *Opt. Express* **19**(6), 5579-5586 (2011).